



UvA-DARE (Digital Academic Repository)

A search for electron antineutrinos associated with gravitational wave events GW150914 and GW151226 using KamLAND

Gando, A.; Decowski, M.P.; The KamLAND Collaboration

DOI

[10.3847/2041-8205/829/2/L34](https://doi.org/10.3847/2041-8205/829/2/L34)

Publication date

2016

Document Version

Final published version

Published in

Astrophysical Journal Letters

[Link to publication](#)

Citation for published version (APA):

Gando, A., Decowski, M. P., & The KamLAND Collaboration (2016). A search for electron antineutrinos associated with gravitational wave events GW150914 and GW151226 using KamLAND. *Astrophysical Journal Letters*, 829(2), [L34]. <https://doi.org/10.3847/2041-8205/829/2/L34>

General rights

It is not permitted to download or to forward/distribute the text or part of it without the consent of the author(s) and/or copyright holder(s), other than for strictly personal, individual use, unless the work is under an open content license (like Creative Commons).

Disclaimer/Complaints regulations

If you believe that digital publication of certain material infringes any of your rights or (privacy) interests, please let the Library know, stating your reasons. In case of a legitimate complaint, the Library will make the material inaccessible and/or remove it from the website. Please Ask the Library: <https://uba.uva.nl/en/contact>, or a letter to: Library of the University of Amsterdam, Secretariat, Singel 425, 1012 WP Amsterdam, The Netherlands. You will be contacted as soon as possible.

UvA-DARE is a service provided by the library of the University of Amsterdam (<https://dare.uva.nl>)



A SEARCH FOR ELECTRON ANTINEUTRINOS ASSOCIATED WITH GRAVITATIONAL-WAVE EVENTS GW150914 AND GW151226 USING KAMLAND

A. GANDO¹, Y. GANDO¹, T. HACHIYA¹, A. HAYASHI¹, S. HAYASHIDA¹, H. IKEDA¹, K. INOUE^{1,2}, K. ISHIDOSHIRO¹, Y. KARINO¹, M. KOGA^{1,2}, S. MATSUDA¹, T. MITSUI¹, K. NAKAMURA^{1,2}, S. OBARA¹, T. OURA¹, H. OZAKI¹, I. SHIMIZU¹, Y. SHIRAHATA¹, J. SHIRAI¹, A. SUZUKI¹, T. TAKAI¹, K. TAMAE¹, Y. TERAOKA¹, K. UESHIMA¹, H. WATANABE¹, A. KOZLOV², Y. TAKEMOTO^{2,3}, S. YOSHIDA³, K. FUSHIMI⁴, A. PIEPKE^{2,5}, T. I. BANKS^{6,7}, B. E. BERGER^{2,7}, B. K. FUJIKAWA^{2,7}, T. O'DONNELL^{6,7}, J. G. LEARNED⁸, J. MARICIC⁸, M. SAKAI⁸, L. A. WINSLOW⁹, E. KRUPCZAK⁹, J. OUELLET⁹, Y. EFREMENKO^{2,10,11}, H. J. KARWOWSKI^{12,13}, D. M. MARKOFF^{12,14}, W. TORNOW^{2,12,15}, J. A. DETWILER^{2,16}, S. ENOMOTO^{2,16}, AND M. P. DECOWSKI^{2,17}

THE KAMLAND COLLABORATION

¹ Research Center for Neutrino Science, Tohoku University, Sendai 980-8578, Japan

² Kavli Institute for the Physics and Mathematics of the universe (WPI), The University of Tokyo Institutes for Advanced Study, The University of Tokyo, Kashiwa, Chiba 277-8583, Japan

³ Graduate School of Science, Osaka University, Toyonaka, Osaka 560-0043, Japan

⁴ Faculty of Integrated Arts and Science, University of Tokushima, Tokushima, 770-8502, Japan

⁵ Department of Physics and Astronomy, University of Alabama, Tuscaloosa, AL 35487, USA

⁶ Physics Department, University of California, Berkeley, CA 94720, USA

⁷ Lawrence Berkeley National Laboratory, Berkeley, CA 94720, USA

⁸ Department of Physics and Astronomy, University of Hawaii at Manoa, Honolulu, HI 96822, USA

⁹ Massachusetts Institute of Technology, Cambridge, MA 02139, USA

¹⁰ Department of Physics and Astronomy, University of Tennessee, Knoxville, TN 37996, USA

¹¹ National Research Nuclear University, Moscow, Russia

¹² Triangle Universities Nuclear Laboratory, Durham, NC 27708, USA

¹³ The University of North Carolina at Chapel Hill, Chapel Hill, NC 27599, USA

¹⁴ North Carolina Central University, Durham, NC 27701, USA

¹⁵ Physics Department at Duke University, Durham, NC 27705, USA

¹⁶ Center for Experimental Nuclear Physics and Astrophysics, University of Washington, Seattle, WA 98195, USA

¹⁷ Nikhef and the University of Amsterdam, Science Park, Amsterdam, The Netherlands

Received 2016 June 29; revised 2016 September 12; accepted 2016 September 14; published 2016 September 30

ABSTRACT

We present a search, using KamLAND, a kiloton-scale anti-neutrino detector, for low-energy anti-neutrino events that were coincident with the gravitational-wave (GW) events GW150914 and GW151226, and the candidate event LVT151012. We find no inverse beta-decay neutrino events within ± 500 s of either GW signal. This non-detection is used to constrain the electron anti-neutrino fluence and the total integrated luminosity of the astrophysical sources.

Key words: gravitational waves – neutrinos

1. INTRODUCTION

With the detection of gravitational waves (GW) by the Advanced Laser Interferometer Gravitational-wave Observatory (LIGO; Abbott et al. 2016c) and high-energy astrophysical neutrinos by IceCube (Aartsen et al. 2015), the era of multi-messenger astronomy has begun in earnest. The combination of these signals with electromagnetic observations offers an unprecedented glimpse into the dynamics of astrophysical phenomena and is already leading to unexpected results.

The first GW event was observed by LIGO on 2015 September 14 at 09:50:45 UTC. Denoted GW150914, this event was observed to have a false alarm rate of less than 1 event per 203,000 years, corresponding to a significance of $>5.1\sigma$ (Abbott et al. 2016c). This likely originated from the coalescence of two black holes at a luminosity distance of 410_{-180}^{+160} Mpc (Abbott et al. 2016c). The second GW event, GW151226, was observed by LIGO on 2015 December 6 at 03:38:53 UTC (Abbott et al. 2016b). GW151226 likely originated from a black hole–black hole (BH–BH) merger that took place at a luminosity distance of 440_{-190}^{+180} Mpc (Abbott et al. 2016b).

We also analyze a GW candidate, dubbed LVT151012 (LIGO–Virgo–Trigger), which occurred on 2015 October 12 at 09:54:43

UTC. While LVT151012 did not cross the threshold required to claim a detection it is unlikely to be a background event, being the only other event reported by LIGO at the time of writing to have a $>50\%$ chance of astrophysical origin (Abbott et al. 2016d). The BH–BH merger suggested by LVT151012 occurred at a luminosity distance of 1100_{-500}^{+500} Mpc (Abbott et al. 2016a).

There is no known mechanism for the production of either neutrinos or electromagnetic waves in a BH–BH merger. While both gamma-ray bursts and neutrino signals can originate from black holes with rapidly accreting disks, the accretion disk is not expected to be present during a BH–BH merger and therefore neither a neutrino signal nor a gamma-ray burst is predicted (Caballero et al. 2012). However, the *Fermi* telescope observed a coincident gamma-ray burst occurring 0.4 s after GW150914 with a false alarm probability of 0.0022 (Connaughton et al. 2016). There is large uncertainty in the origin region but it is consistent with that reported by LIGO (Connaughton et al. 2016). The statistical treatment has been debated and the event may be consistent with background (Greiner et al. 2016). If this burst truly originates from the same black hole merger as GW150914 it could imply that some accretion disk remained during the merger, thus motivating a multi-messenger analysis including neutrinos of all energies.

In this paper, we search for correlations between these GW events and electron antineutrinos of a few tens of MeV, and place constraints on the neutrino fluence and luminosity. This work is complementary to the multi-messenger analysis performed by IceCube and ANTARES at higher energies, which did not find any neutrino events correlated with GW150914 with sufficient significance (Adrian-Martinez et al. 2016).

2. KAMIOKA LIQUID SCINTILLATOR ANTI-NEUTRINO DETECTOR (KAMLAND)

KamLAND is optimized to search for \sim MeV neutrinos and antineutrinos. KamLAND is located under 2700 m water-equivalent of vertical rock, below Mt. Ikenoyama in the Gifu prefecture of Japan. KamLAND consists of an 18 m diameter stainless steel sphere that has 1325 17 inch and 554 20 inch photomultiplier tubes mounted on its inside surface. The sphere contains a 13 m diameter EVOH/nylon outer balloon surrounded by pure mineral oil. This outer balloon encloses 1 kton of highly purified liquid scintillator. Surrounding the stainless steel sphere is a cylindrical 3.2 kton water-Cherenkov detector to provide shielding and allow cosmic-ray muon identification. Additional details of KamLAND are summarized in Suzuki (2014). During the period corresponding to the detection of GW150914 and LVT151012, a 3.08 m diameter transparent nylon inner balloon (“mini-balloon”) containing 13 tons of Xe-loaded liquid scintillator had been placed at the center of the detector (Gando et al. 2012b). At the time that GW151226 was detected, the mini-balloon had been removed and KamLAND was in its normal configuration.

In this analysis, we will focus on the detection of antineutrinos through the inverse beta-decay (IBD) reaction: $\bar{\nu}_e + p \rightarrow e^+ + n$. This process is characterized by a delayed coincidence event pair signature. The prompt event is a combination of the deposition of the kinetic energy of the positron and its subsequent annihilation into gamma-rays. This event encodes the energy of the incoming anti-neutrino. This annihilation occurs on a very short timescale. Because the angular distribution of the positron emission and the subsequent scintillation light are isotropic, KamLAND has no directional sensitivity. The delayed event is the emission of a gamma-ray when the neutron captures on carbon or a proton, with a mean neutron capture time of $207.5 \pm 2.8 \mu\text{s}$ (Abe et al. 2010). The detection of this second gamma-ray completes the delayed coincidence pair.

KamLAND’s main background source depends on the energy region. At energies of a few MeV, reactor neutrinos and geoneutrinos dominate for standard analysis (Gando et al. 2013). For the purposes of this coincidence search we have used the maximum possible detector volume and removed filters that screen out accidental radiation from the support structure. Thus, the background is dominated by low-energy events caused by accidental coincidences of natural radioactivity. The majority of the remaining low-energy backgrounds are from reactor neutrinos and geoneutrinos; the event rate of reactor neutrinos was about 0.1–0.2 events per day during this period, and the geoneutrino background rate was about 0.1 event per day. Above \sim 7.5 MeV, the majority of the background comes from neutral current interactions with atmospheric neutrinos (Gando et al. 2012a). This background is effectively constant up to \sim 100 MeV. For a more detailed discussion of KamLAND’s backgrounds, please see Asakura

et al. (2015) and Gando et al. (2013). KamLAND’s lower energy threshold gives it an advantage in this low-energy neutrino range compared to the IceCube and Super-Kamiokande detectors.

3. COINCIDENCE SEARCH

The detection of the gamma-ray burst by the *Fermi* telescope suggests that the BH–BH merger detected by LIGO might have retained its accretion disk. The spectrum of accretion disk neutrinos around a single black hole is expected to peak around 10 MeV, with the majority falling well below 100 MeV (Caballero et al. 2012 and McLaughlin & Surman 2007). In the absence of a mechanism for neutrino production by a BH–BH merger, we consider the single BH accretion model and search for IBD events with visible energies between 0.9 and 100 MeV, corresponding to neutrino energies between 1.8 and 111 MeV. We choose a coincidence window of ± 500 s by selecting the largest expected time gap between GW events and high-energy neutrino events described in Baret et al. (2011). We use the standard KamLAND event selection (Abe et al. 2010). This restricts the analysis to $R < 6$ m to remove backgrounds from the main balloon. It also applies a veto of 2 s within a 3 m cylinder or a 2 s full detector veto following muon events depending on the quality of the muon track reconstruction to reduce background due to the long-lived muon spallation product ${}^9\text{Li}/{}^8\text{He}$ (Abe et al. 2010). The muon veto leads to a difference in the livetime-to-real-time ratio, where livetime is defined as the period of time during which the detector was sensitive to $\bar{\nu}_e$ and includes corrections for calibration periods, detector maintenance, and other factors. The average livetime-to-real-time ratio is $\epsilon_{\text{live}} = 0.89$ for the two KamLAND runs containing GW150914 and LVT151012. The livetime-to-real-time ratio is $\epsilon_{\text{live}} = 0.81$ for the run containing GW151226.

Two changes were made to the standard KamLAND criteria (Gando et al. 2013); we removed the mini-balloon cut and the likelihood selection. These cuts increase the background due to the mini-balloon and main balloon. The total detection efficiency of $\epsilon_s = 0.93$ was then estimated from Monte Carlo simulation.

We searched for events that fell within a 500 s window of the two GW events GW150914 and GW151226, and the candidate event LVT151012. No events were found within the target window of GW150914 (Figure 1), GW151226 (Figure 2), or LVT151012 (Figure 3). The closest neutrino candidate event to either GW event occurred 1124 s prior to LVT151012. This event was at a very low energy of 1.4 MeV and occurred near the nylon corrugated pipe that supports the mini-balloon. Therefore, this event was consistent with the expected background and may have been caused by contamination from the mini-balloon support structure. There were no other events within three hours of LVT151012. The closest neutrino candidate to GW151226 occurred about 40 minutes away and was of less than 3 MeV. The closest two neutrino candidate events to GW150914 occurred about 2.5 hours away from the event and were both less than 2 MeV. Therefore all adjacent observed events are likely background.

The background rate for GW150914 and LVT151012 is given by the average number of IBD events under 100 MeV occurring per second of detector livetime between 2015 April and early 2015 November. KamLAND’s background during this period is $(2.02 \pm 0.04) \times 10^{-4}$ events per second of

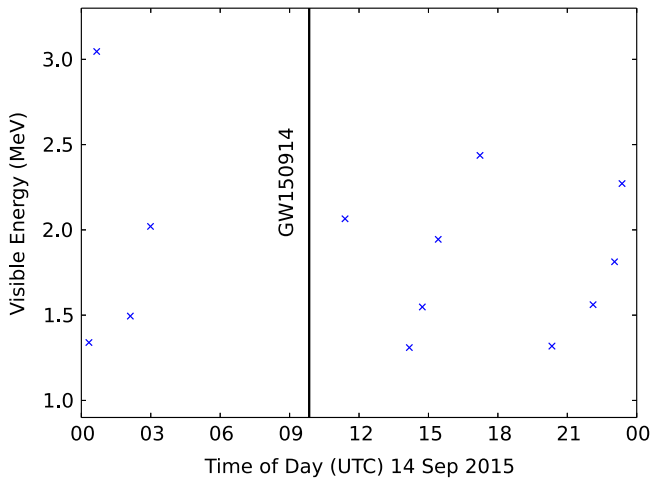


Figure 1. Neutrino events between 0.9 and 100 MeV visible energy occurring on 2015 September 14. The highest-energy event in this time span was at 3.05 MeV. The time of GW150914 is marked. There were no events within 500 s of GW150914.

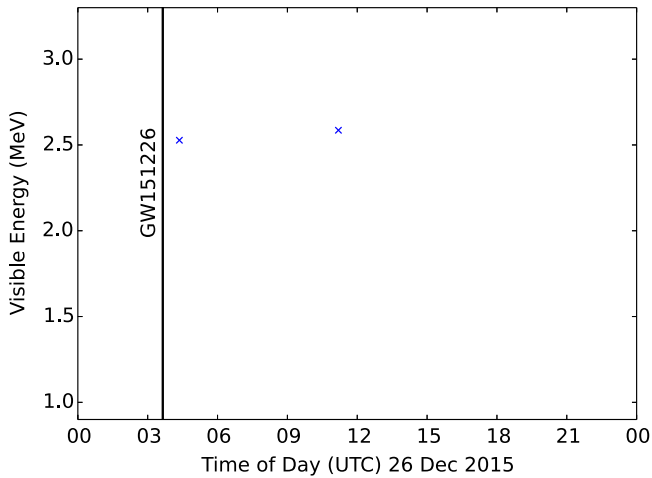


Figure 2. Neutrino events between 0.9 and 100 MeV visible energy occurring on 2015 December 6. The highest-energy event in this time span was at 2.58 MeV. The time of GW151226 is marked. There were no events within 500 s of GW151226. The closest event occurred approximately 40 minutes after GW151226 and was consistent with the background.

lifetime. This corresponds to 0.18 events in a 1000 s real-time window. The accidental coincidence rate during this period was 1.7×10^{-4} events s^{-1} ; thus accidental coincidences dominate the background.

We checked the stationarity of the background rate and found that the event rate was statistically constant. Using the previously calculated background rate and the detection of no coincidence events, using the Feldman Cousins method (Feldman & Cousins 1998), we determined that the 90% confidence limit on the number of detected neutrinos is calculated from the background rate to be $N_{90} = 2.26$.

The background rate for GW151226 is given by the average number of IBD events under 100 MeV occurring per second of detector livetime between 2015 December 23 and 2016 January 4. This time period was chosen to avoid the period during which KamLAND underwent some refurbishment work. The background rate during this period was found to be $(3.4 \pm 0.6) \times 10^{-5}$ events per second of livetime, giving $N_{90} = 2.41$ (Feldman & Cousins 1998). This background

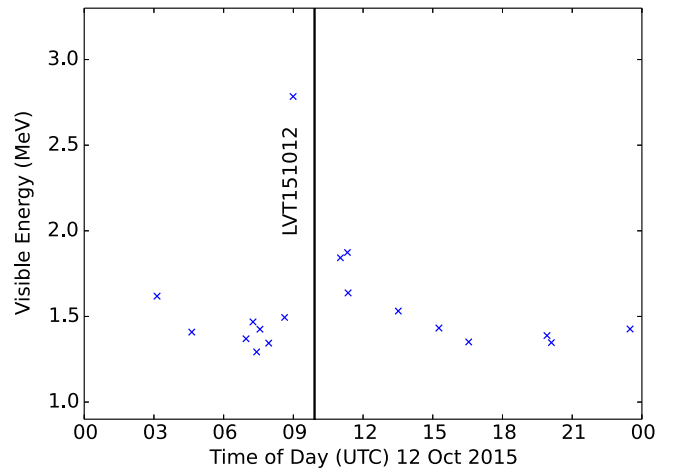


Figure 3. Neutrino events between 0.9 and 100 MeV visible energy occurring on 2015 October 12. The highest-energy event in this time span was at 2.78 MeV. The time of LVT151012 is marked. There were no events within 500 s of LVT151012. The closest event occurred at 1124 s prior to LVT151012 and was consistent with the background.

corresponds to 0.03 events per 1000 s of real time. We expect this background to be lower than that for the period from April to November because the mini-balloon, a source of background contamination, was not in the detector during this time period. The accidental coincidence rate during this period was 2.6×10^{-5} events s^{-1} .

4. FLUENCE AND LUMINOSITY

We translate our Feldman Cousins upper limit into a fluence upper limit at the detector. This fluence upper limit is given in neutrinos per cm^2 by

$$F_{UL} = \frac{N_{90}}{N_T \epsilon_{\text{live}} \epsilon_s \int \sigma(E_\nu) \lambda(E_\nu) dE_\nu}, \quad (1)$$

where N_T is the total number of target protons in the fiducial volume, ϵ_{live} is the mean livetime-to-real-time ratio, ϵ_s is the total detection efficiency, $\sigma(E_\nu)$ is the total neutrino cross-section, and $\lambda(E_\nu)$ is the normalized neutrino energy spectrum (Fukuda et al. 2002). The estimated target number for KamLAND is $N_T = (5.98 \pm 0.13) \times 10^{31}$. The neutrino IBD cross-section was taken from Strumia & Vissani (2003). The quenching effect and the effect of energy resolution were considered and found to be negligible; thus these effects are not included in Equation (1).

The electron anti-neutrino fluence upper limit without oscillation and assuming a monochromatic spectrum is given by

$$F_{UL}(E_\nu) = \frac{N_{90}}{N_T \sigma(E_\nu) \epsilon_{\text{live}} \epsilon_s}. \quad (2)$$

The resulting upper limit on fluence ranges from about 10^{13} cm^{-2} for a neutrino energy of 1.8 MeV to about 10^8 cm^{-2} for a neutrino energy of 100 MeV. The monochromatic spectrums for electron anti-neutrino fluence upper limit are shown in Figure 4.

In the absence of a BH–BH merger-specific neutrino energy spectrum prediction, we choose the spectrum given by the normalized pinched Fermi–Dirac distribution for zero chemical

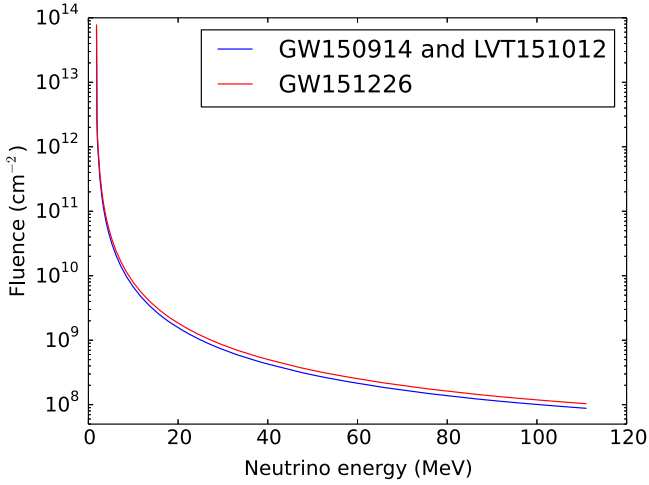


Figure 4. Upper limit of electron anti-neutrino fluence at the detector for each energy between 0.9 and 100 MeV, assuming a monochromatic spectrum. The spectrums for GW150914 and LVT151012 are the same, due to their shared background rate, and thus they share a fluence upper limit. The background rate for GW151226 is about an order of magnitude lower and thus its fluence upper limit is a bit higher.

potential and pinching factor $\eta = 0$:

$$\lambda_{\text{FD}}(E) = \frac{1}{T^3 F_2(\eta)} \frac{E^2}{e^{E/T-\eta} + 1}, \quad (3)$$

where the complete Fermi–Dirac integral $F_n(\eta)$ is given by

$$F_n(\eta) = \int_0^\infty \frac{x^n}{e^{x-\eta} + 1} dx. \quad (4)$$

The temperature is given by $T = \langle E \rangle / 3.15$. We choose $E = 12.7$ MeV from Caballero et al. (2016); the small change in average energies between accretion disk models had a negligible impact on the result.

Substituting this spectrum into (1) and performing the integration between electron anti-neutrino energies of $E_{\text{min}} = 1.8$ MeV and $E_{\text{max}} = 111$ MeV, we get a total integrated electron anti-neutrino fluence for both GW150914 and LVT151012 of

$$F \leq 3.1 \times 10^9 \text{ cm}^{-2}. \quad (5)$$

The total integrated electron anti-neutrino fluence for GW151226 is

$$F \leq 3.6 \times 10^{10} \text{ cm}^{-2}. \quad (6)$$

There is a large uncertainty in the distance for all of GW150914, GW151226, and LVT151012, so the total energy upper limit is here displayed as a function of the true distance to the source, D_{GW} . The electron anti-neutrino total energy upper limits without oscillation for GW150914, GW151226, and LVT151012 are thus given by

$$E_{\text{GW150914}} \leq 1.26 \times 10^{60} \left(\frac{D_{\text{GW}}}{410 \text{ Mpc}} \right)^2 \text{ erg} \quad (7)$$

and

$$E_{\text{GW151226}} \leq 1.71 \times 10^{60} \left(\frac{D_{\text{GW}}}{440 \text{ Mpc}} \right)^2 \text{ erg} \quad (8)$$

and finally,

$$E_{\text{LVT151012}} \leq 9.06 \times 10^{61} \left(\frac{D_{\text{GW}}}{1100 \text{ Mpc}} \right)^2 \text{ erg}. \quad (9)$$

This limit complements the upper limit on total energy found by the IceCube-ANTARES joint analysis, since the results are based on a different energy region. The IceCube-ANTARES upper limit on total radiated energy is

$$E_{\nu, \text{tot}}^{\text{ul}} \sim 10^{52} - 10^{54} \left(\frac{D_{\text{GW}}}{410 \text{ Mpc}} \right)^2 \text{ erg} \quad (10)$$

for neutrinos in the \gg GeV energy range (Adrian-Martinez et al. 2016).

The neutrino event rate scales as a function of the disk’s mass accretion rate. For current detector masses (for example, Super-Kamiokande), the number is $\sim 10,000$ events at 10 kpc, so accounting for the $1/r^2$ scaling with distance, Super-Kamiokande may see one event from a black hole merger at 1 Mpc (Caballero et al. 2016).

Unfortunately, our results do not constrain any viable accretion disk model. Caballero et al. (2016) predicts approximately 500 events per kiloton at 10 kpc for accretion rates on the order of $5M_\odot \text{ s}^{-1}$. At 1000 Mpc a 100 gigaton detector would be required. This detector would be similar to IceCube (Adrian-Martinez et al. 2016), but would be instrumented more densely to obtain a ~ 10 MeV energy threshold.

5. CONCLUSION

No coincident neutrino events were found within 500 s of either GW150914, GW151226, or LVT151012. We determined a monochromatic fluence upper limit, as well as an upper limit on the source luminosity for each GW event and candidate GW event using the standard source model. This places a bound on the total energy released as low-energy neutrinos. The lack of coincident IBD events detected by KamLAND further supports the conclusion by the Dark Energy Survey Collaboration that GW150914 was not a core-collapse supernova in the Large Magellanic Cloud (Annis et al. 2016).

As Advanced LIGO continues its operation, we can expect many more opportunities to perform multi-messenger searches and look for coincidence neutrinos. The more complete understanding of the source dynamics provided by such a search grants us an exciting opportunity to explore black holes, supernova, and other elusive astrophysical phenomena.

We are indebted to the LIGO Scientific Collaboration for their gravitational-wave observations. KamLAND is supported by MEXT KAKENHI Grant Numbers 26104002, 26104007; the World Premier International Research Center Initiative (WPI Initiative), MEXT, Japan; and under the U.S. Department of Energy (DOE) grants no. DE-FG03-00ER41138, DE-AC02-05CH11231, and DE-FG02-01ER41166, as well as other DOE and NSF grants to individual institutions, and Stichting Fundamenteel Onderzoek der Materie (FOM) in the Netherlands. The Kamioka Mining and Smelting Company has provided services for activities in the mine. We thank the support of NII for SINET4.

REFERENCES

- Aartsen, M. G., Abraham, K., Ackermann, M., et al. 2015, *ApJ*, 809, 98
- Abbott, B. P., Abbott, R., Abbott, T. D., et al. 2016a, arXiv:1602.03839
- Abbott, B. P., Abbott, R., Abbott, T. D., et al. 2016b, *PhRvL*, 116, 241103
- Abbott, B. P., Abbott, R., Abbott, T. D., et al. 2016c, *PhRvL*, 116, 061102
- Abbott, B. P., Abbott, R., Abbott, T. D., et al. 2016d, arXiv:1602.03842
- Abe, S., Enomoto, S., Furuno, K., et al. 2010, *PhRv*, C81, 025807
- Adrian-Martinez, S., Albert, A., André, M., et al. 2016, *PhRvD*, 93, 122010
- Annis, J., Soares-Santos, M., Berger, E., et al. 2016, *ApJL*, 823, L34
- Asakura, K., Gando, A., Gando, Y., et al. 2015, *ApJ*, 806, 87
- Baret, B., Bartos, I., Bouhou, B., et al. 2011, *APh*, 35, 1
- Caballero, O. L., McLaughlin, G. C., & Surman, R. 2012, *ApJ*, 745, 170
- Caballero, O. L., Zielinski, T., McLaughlin, G. C., & Surman, R. 2016, *PhRv*, D93, 123015
- Connaughton, V., Burns, E., Goldstein, A., et al. 2016, *ApJL*, 826, L6
- Feldman, G. J., & Cousins, R. D. 1998, *PhRv*, D57, 3873
- Fukuda, S., Fukuda, Y., Ishitsuka, M., et al. 2002, *ApJ*, 578, 317
- Gando, A., Gando, Y., Hanakago, H., et al. 2012b, *PhRvC*, 85, 045504
- Gando, A., Gando, Y., Hanakago, H., et al. 2013, *PhRvC*, 88, 033001
- Gando, A., Gando, Y., Ichimura, K., et al. 2012a, *ApJ*, 745, 193
- Greiner, J., Burgess, J. M., Savchenko, V., & Yu, H. F. 2016, arXiv:1606.00314
- McLaughlin, G. C., & Surman, R. 2007, *PhRv*, D75, 023005
- Strumia, A., & Vissani, F. 2003, *PhL*, B564, 42
- Suzuki, A. 2014, *EPJC*, C74, 3094